Ultrasound Velocity Measurements in High-Chromium Steel Under Plastic Deformation

Aleksey Lunev [1,2,a], Anna Bochkareva [1,2,b], Svetlana Barannikova [1,3,4,c], Lev Zuev [1,3,d]

[1]Institute of Strength Physics & Materials Science, SB RAS, 2/4 Akademicheskii Ave., Tomsk, 634055, Russia
[2]National Research Tomsk Polytechnic University, 30 Lenina ave., Tomsk, 634050, Russia
[3]National Research Tomsk State University, 36 Lenin Ave., Tomsk, 634050, Russia
[4]Tomsk State University of Architecture and Building, 2 Solyanaya Ave., 634003, Tomsk, Russia

e-mail: [a]agl@ispms.tsc.ru, [b]avb@ispms.tsc.ru, [c]bsa@ispms.tsc.ru (corresponding author), [d]lbz@ispms.tsc.ru

Abstract. In the present study, the variation of the propagation velocity of ultrasound in the plastic deformation of corrosion-resistant high-chromium steel 40X13 with ferrite-carbide (delivery status), martensitic (quenched) and sorbitol (after high-temperature tempering) structures have beem studied/ It is found that each state shows its view of the loading curve. In the delivery state diagram loading is substantially parabolic throughout, while in the martensitic state contains only linear strain hardening step and in the sorbitol state the plastic flow curve is three-step. The velocity of ultrasonic surface waves (Rayleigh waves) was measured simultaneously with the registration of the loading curve in the investigated steel in tension. It is shown that the dependence of the velocity of ultrasound in active loading is determined by the law of plastic flow, that is, the staging of the corresponding diagram of loading. Structural state of the investigated steel is not only changing the type of the deformation curve under uniaxial tension, but also changes the nature of ultrasound speed of deformation.

Introduction

The commonly accepted concepts of the process of plastic deformation are based on the data testifying that it occurs in stages [1], and the adequacy of the models developed for describing this process implies a strict correspondence between the stages and the governing microscopic mechanisms. The determination of the boundaries of these stages and the corresponding mechanisms presents a complicated problem, especially for polycrystals, because, in most cases, reliable and informative external manifestations of the changes in the deformation mechanisms are absent. For such purposes, the data on the integral characteristics of the material, e.g., magnetization and electric resistance, can be useful. They are especially valuable, because, in contrast to microscopic studies, they can be

obtained immediately in the course of mechanical tests without any additional operations related to the preparation of special samples for the analysis.

From this point of view, acoustical methods of studying the properties of solids are quite promising [2-4]. In addition to the commonly used effects such as the acoustic emission from mechanically loaded samples or the amplitude dependence of internal friction, which can be interpreted on the basis of specially developed theoretical models, it is possible to use a more easily measured characteristic, namely, the velocity of ultrasound propagation V. Rayleigh waves, one kind of surface acoustic waves, are ideally suited to surface inspection problems [5]. The penetration depth depends on the frequency of Rayleigh waves. Approximately, the penetration depth is in the order of the wavelength [6]. Rayleigh waves with higher frequencies are more influenced by the surface layer, because they have a lower penetration depth. Damage usually tends to initiate and to concentrate at the surface. For the study of surface imperfections and damage, Rayleigh waves that form and propagate along boundaries, are better suited than body waves to study surface process [7].

It was shown [8] that in the course of plastic flow the propagation velocity of ultrasonic surface waves (Rayleigh waves) in the material changes, the dependence $V(\varepsilon)$ having a complicated N shape. In the present paper we present data on the dependence of V on the magnitude of the stress σ acting during deformation of high-chromium steel. The material possesses an appealing combination of strength and plastic properties, corrosion resistance in atmospheric, water-vapor, aquatic, and (on numerous occasions) acid environments, and is compositionally simple. This has led to its widespread use for production of critical machine parts and structural members. Certification of this kind of materials makes it essential to determine the following characteristics: ductility margin, life time, and fracture mode, all being dependent in many respects on strain-localization patterns [9, 10]. The deformation behavior of high-chromium steel was investigated in [11]. The variation of the propagation velocity of ultrasound in the plastic deformation of corrosion-resistant high-chromium steel with ferrite-carbide (delivery status), martensitic (quenched) and sorbitol (after high-temperature tempering) structures have been studied.

Materials and experimental methods

The test material was high-chromium stainless steel (0.4%C–0.6%Si–0.55%Mn–12.5%Cr). The specimens were configured as dog bones with gage section measuring 50×10×2 mm. The test pieces were cut out from sheet steel along the rolling direction. The material was examined with ferrite-carbide (delivery status), martensitic (quenched) and sorbitol (after high-temperature tempering) structures. The specimens were homogenized at T = 1320 K for 3 hrs and subjected to fast air cooling to provide martensitic structure with a small amount of chromium carbides. On high-temperature tempering from T = 870 K for 3 hrs and furnace cooling, sorbitic structure (ferrite and carbides) was generated. The structure of steel in various types of heat treatment was studied by using optical and atomic force microscopy. The specimens thus prepared were subjected to uniaxial tension at room temperature at the rate $6.67 \cdot 10^{-5}$ s^{-1} (0.2 mm/min).

The velocity of ultrasonic surface waves (Rayleigh waves) was measured simultaneously with the registration of the loading curve in the investigated steel in tension in a LFM-125 testing machine using an OWON RDS6062S device. The principle for measuring the velocity of propagation of Rayleigh waves is based on the pulse autocirculation method [12]. The error of the measurement amounts to $2 \cdot 10^{-4}$, and operation with the instrument does not require any special skills on the part of the operator. The basic principle of the autocirculation method consists of setting up a closed circuit to transmit the pulses. A radiating piezoelectric transducer, when acted upon by a short electric pulse, generates an acoustic wave in the sample. The wave traveling from the transmitting piezoelectric transducer to the receiving piezoelectric transducer is converted back into an electrical signal and again arrives at the radiating transducer. Hence, keeping the distance between the transducers fixed, the frequency at which a pulse appears at a certain point of the circuit will depend on the time taken for the acoustic signal to travel through the sample and the delay in the circuit. Since the delay in the circuit is negligibly small compared with the propagation time of the acoustic wave in the sample, the

autocirculation frequency will characterize the velocity of propagation of the ultrasonic wave in the sample. In this case the Rayleigh surface waves have a frequency of 5 MHz.

The ultrasonic sensor, placed on the object being investigated, has two inclined piezoelectric transducers, situated at a fixed distance from one another, called the base. The inclination of the piezoelectric transducers is chosen in such a way that a surface Rayleigh wave is generated in the object. For reliable measurement of the velocity, it is necessary to ensure that the contact with the metal of the article being monitored is clean, the surface must be smooth, and the sensor must be pressed tightly in position. Acoustic contact with the piezoelectric transducer is provided by a no aggressive liquid lubrication, for example, transformer oil. One must bear in mind that the space between the piezoelectric transducers must remain dry and clean.

Experimental results

The stress-strain curves for the material are shown in Fig. 1. The work-hardening modes for the delivery status (1), quenched steel (2) and that subjected to quenching and high-temperature tempering (3) are seen to be essentially different. In the deforming sample of the original alloy (1), the onset of necking takes place, which is a forerunner of viscous fracture. The quenched steel (2) exhibits pseudo brittle fracture without distinct necking. In the tempered steel (3), a well-pronounced neck is formed, and the descending branch of the curve indicates that up to 2% of the total strain is built up for the fracture percent elongation δ = 9.6%.

The stress-strain curve for a polycrystalline material can be described by the Lüdwick relation [1]

$$\sigma = \sigma_0 + K\varepsilon^n \qquad (1)$$

where K is the coefficient of deformation hardening and n is the exponent of deformation hardening. The strain exponent n has different values in different portions of the stress-strain curve and changes in a stepwise manner depending on the degree of strain. To each of the deformation stages correspond particular constant values of n and K.

Using the method reported in [11], the loading curve can be represented in the system of functional logarithmic coordinates as $\ln(s - s_0) = f(\ln e)$ (here s is the true stress which takes no account of reduction in the work cross-section and e is the true deformation). This enables individual segments to be singled out on the curve for a constant value of the exponent n, which varies discretely on going from one segment to the next. All the loading diagrams obtained in this study were analyzed by the above method.

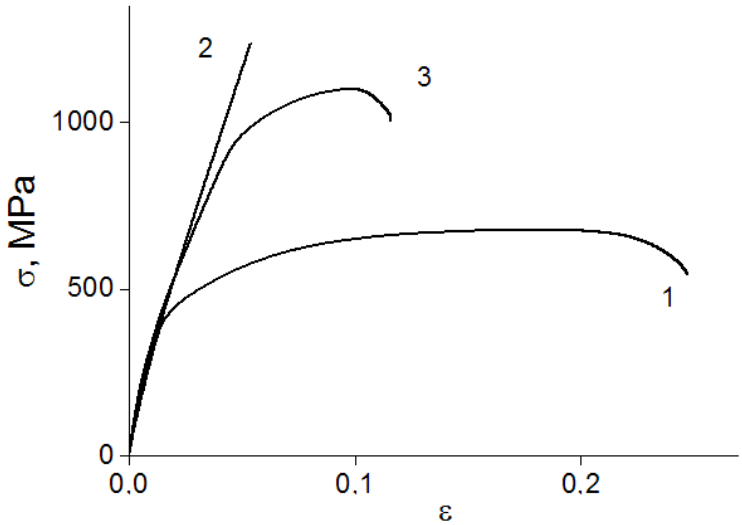

Fig. 1. Stress-strain curves for high-chromium steel: 1 – delivery status; 2 – quenched state; 3 – tempered state

The quantitative data on mechanical characteristics and deformation stages of alloys are listed in the Table 1 and Table 2. The deformation curves plotted for the original alloy (1) were represented in functional logarithmic coordinates. One rectilinear segment is distinguished on the flow curve for strains ε in the range 1.4-6.8% for a constant value $n \approx ½$. This segment corresponds to the parabolic work hardening stage.

Table 1. Mechanical characteristics of high-chromium stainless steel (1 – delivery status; 2 – quenched state; 3 – tempered state)

	$\sigma_{0.2}$ [MPa]	σ_B [MPa]	δ [%]	HV [MPa]	V_0 [m/s]
1	420.0	676.6	22.7	2060	3067
2	348.5	1233.4	1.97	3880	2958
3	278.6	1098.3	9.6	3498	3034

Footnotes: $\sigma_{0.2}$ – proof stress; σ_B – ultimate stress; δ – relative elongation to rupture; HV - microhardness values; V_0 - velocity of Rayleigh waves in the unstressed sample.

Thus the stress-strain curve for the quenched steel has been found to include a linear-hardening stage for strains $0.9 \le \varepsilon \le 4.5\%$ followed by a stage with constantly changing values of n and K (Fig. 1). The stress-strain curve for the tempered steel exhibits three deformation stages (Fig. 1). These are a linear-hardening stage ($1.9 \le \varepsilon \le 4.1\%$), a Taylor parabolic work-hardening stage ($5.3 \le \varepsilon \le 7.1\%$) with $n \approx ½$ and a prefracture stage ($7.7 \le \varepsilon \le 9.5\%$) with $n = 0.3$. The data agree with the results of previous studies [11].

It has been established [8] that the velocity of propagation of an ultrasonic wave in a sample deformed by stretching depends on the overall strain, the stress time and the structure of the material. The analysis of the dependences of the velocity V on the total strain ε and the actual stress σ for deformations up to fracture revealed a number of interesting effects (Fig. 2, Fig. 3). It was found that the ultrasonic velocity considerably varies with tension, and the dependences $V(\varepsilon)$ and $V(\sigma)$ are fairly complicated. For example, the curve $V(\varepsilon)$ obtained for tempered state and shown in Fig. 2 c is *N*-shaped with three well-defined stages [8]. Such a shape testifies to the difference between the mechanisms governing the relation between V and ε in the corresponding intervals of plastic deformation.

Table 2. Deformation stages of high-chromium stainless steel (1 – delivery status; 2 – quenched state; 3 – tempered state)

Material/State	Linear-hardening stage $\sigma \sim \varepsilon$		Taylor parabolic work-hardening stage $\sigma \sim \varepsilon^{1/2}$		Prefracture stage $\sigma \sim \varepsilon^{1/3}$	
	ε_{init} [%]	ε_{fin} [%]	ε_{init} [%]	ε_{fin} [%]	ε_{init} [%]	ε_{fin} [%]
1	-	-	1.4	6.8	-	-
2	0.9	4.5	-	-	-	-
3	1.9	4.1	5.3	7.1	7.7	9.5

In these investigations, attention was paid to the way in which the velocity of ultrasonic waves depends on the stress. Using dimensionless values of the velocity and the stress and approximating the separate stages by linear functions, we obtain the generalized relation [8]

$$\frac{V}{V_0} = \alpha_i \frac{\sigma}{\sigma_B} + \beta_i, \qquad (2)$$

where V_0 is the velocity of Rayleigh waves in the unstressed sample, m/sec; α_i and β_i are empirical quantities, independent of the material; $i = 1, 2$ is the number of the linear part in Fig. 3; and σ_B is the

tensile strength of the material being investigated, MPa. The calculated values of α_i and β_i for sections 1, 2 and 3 are listed in the Table 3.

The typical dependences V/V_0 and σ/σ_B shown in Fig. 3 for delivery status (1) and tempered state (3) have three stages, and for the quenched steel (2) - one stage. The linear character of the relation between V and σ at each stage is interesting. Similar three-stage dependences $V(\sigma)$ were obtained for the other materials studied in the course of the experiments described [8].

Table 3. Empirical quantities α_i and β_i for Eq. (2) for delivery status (1), quenched state (2), tempered state (3) of high-chromium stainless steel

Segment	Delivery status (1)		Quenched state (2)		Tempered state (3)	
	α_i	β_i	α_i	β_i	α_i	β_i
1	$-9.4\cdot10^{-4}$	1	$-4.37\cdot10^{-4}$	1	$5.97\cdot10^{-4}$	1
2	$-1.29\cdot10^{-2}$	1.008			$-3.42\cdot10^{-3}$	1.002
3	$-5.46\cdot10^{-2}$	1.048			$-4.07\cdot10^{-2}$	1.034

It follows from (2) that

$$\sigma_{Б} = \alpha_i \sigma / (V/V_0 - \beta_i) \quad (3)$$

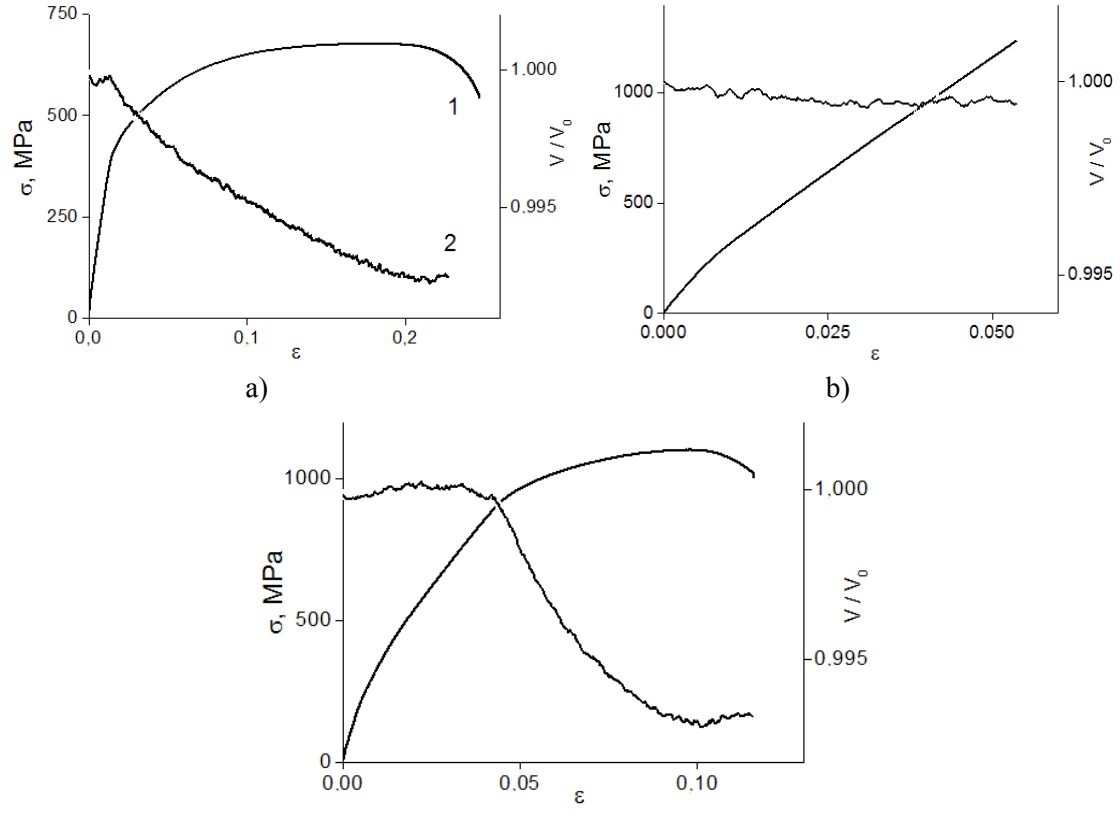

Figure 2. Stress–strain curve of the plastic flow (1) for delivery status (a), quenched state (b), tempered state (c) of high-chromium stainless steel and the dependence of the velocity of ultrasound propagation against the total strain (2)

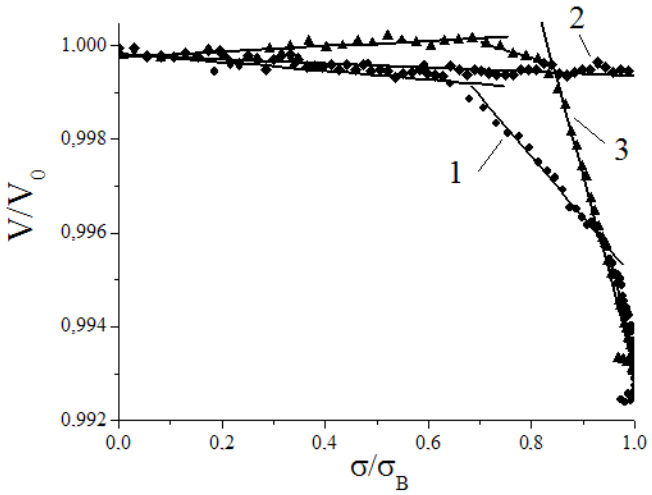

Figure 3. The dependence of the velocity of ultrasound propagation against the acting stresses for delivery status (1), quenched state (2), tempered state (3) of high-chromium stainless steel

Equation (3) can be used to estimate the tensile stress for small plastic deformations long before the sample fractures. Hence, in order to determine σ_B, it is sufficient to measure the velocity of ultrasonic waves for stresses in the sample in the range $\sigma_{0.2} < \sigma < 0.6\sigma_B$ (where $\sigma_{0.2}$ is the tensile strength), i.e., in the section of small plastic deformations.

Summary
The velocity of ultrasonic surface waves (Rayleigh waves) was measured simultaneously with the registration of the loading curve of high-chromium steel subjected with ferrite-carbide (delivery status), martensitic (quenched) and sorbitol (after high-temperature tempering) structures. In the delivery state diagram loading is substantially parabolic throughout, while in the martensitic state contains only linear strain hardening step and in the sorbitol state the plastic flow curve is three-step. It is shown that the dependence of the velocity of ultrasound in active loading is determined by the law of plastic flow, that is, the staging of the corresponding diagram of loading. Structural state of the investigated steel is not only changing the type of the deformation curve under uniaxial tension, but also changes the nature of ultrasound speed of deformation. The data obtained from this investigation are of practical use for developing theoretical foundations of plastic working of high-chromium steel. This can provide, among other things, a reliable choice of limiting degrees of strain for cold rolling of sheet slabs and tubular billets. The proposed method can be used to estimate the tensile strength of high-chromium steels before they fracture.

Acknowledgment
The work was performed in the frame of the Tomsk State University Academic D.I. Mendeleev Fund Program and the Program of Fundamental Research of State Academies of Sciences for the period 2014-2020 yrs.

References
[1] J Pelleg, Mechanical properties of materials, Springer, Dordrecht, Heidelberg, New York, London, 2013.
[2] M Kobayashi, S. Tang, S. Miura, K. Iwabuchi, S. Oomori, H. Fujiki, Ultrasonic nondestructive material evaluation method and study of texture and cross slip effects under simple and pure shear states, Int. J. Plast. 19 (2003) 771–804.
[3] V V Mishakin, S Dixon, M D G Potter, The use of wide band ultrasonic signals to estimate the stress condition of materials, J. Phys. D: Appl. Phys. 39 (2006) 4681-4687.

[4] V V Murav'ev, L V Volkova, E N Balobanov, Estimation of residual stresses in locomotive wheel treads using the acoustoelasticity method, Rus. J. Nondestr. Test. 49 (2013) 382-386.
[5] J D N Cheeke, Fundamentals and applications of ultrasonic waves, CRC Press, Boca Raton, 2002
[6] D Schneider, B Brenner, T Schwarz, Characterization of laser hardened steels by laser induced ultrasonic surface waves, J. Nondestr. Eval. 14 (1995) 21–9.
[7] A Zerwer, M A Polak, J C Santamarina, Wave propagation in thin plexiglas plates: implications for Rayleigh waves, NDTE Int. 33 (2000) 33–41.
[8] L B Zuev, B S Semukhin, A G Lunev, The use of measurements of the velocity of ultrasound to determine the stress-strain state of metal articles, Meas. Techn. 53 (2010) 439-443.
[9] L B Zuev, V I Danilov, S A Barannikova, V V Gorbatenko, Autowave model of localized plastic flow of solids, Phys. Wav. Phen. 17 (2009) 1–10.
[10] L B Zuev, S A Barannikova, Experimental study of plastic flow macro-scale localization process: pattern, propagation rate, dispersion, Int. J. Mech. Sci. 88 (2014) 1-8.
[11] V I Danilov, D V Orlova, L B Zuev, G V Shlyakhova, Special features of the localized plastic deformation and fracture of high-chromium steel of the martensitic class, Rus. Phys. J. 52 (2009) 525-531.
[12] R Truell, C Elbaum, B Chick, Ultrasonic Methods in Solid State Physics, Academic Press, New York, 1969.